

Variability of biogeochemical processes and physical transport in a partially stratified estuary: a box-modeling analysis

Jeremy M. Testa*, W. Michael Kemp

University of Maryland, Center for Environmental Science, Horn Point Laboratory, 2020 Horns Point Road, Cambridge, Maryland 21613, USA

ABSTRACT: Regional, seasonal, and interannual variations of freshwater inputs, biogeochemical transformations, and pelagic–benthic interactions were examined in the Patuxent River estuary. Monthly rates of net biogeochemical production (or consumption) and physical transport of carbon, oxygen, and nutrients were calculated for 6 estuarine regions using data-constrained salt- and water-balance computations (box model) with hydrologic and water quality data. Assuming fixed stoichiometry for O₂, carbon, and silicate, we derived estimates of particulate organic carbon (POC) sinking and net diatom growth. Our results indicate that nutrients delivered from the watershed to the estuary during winter and spring supported >100% of the spring phytoplankton bloom. The spring bloom, which subsequently sinks across the pycnocline to the bottom layer, was decomposed in May–September to support 50 to 90% of annual bottom-layer NH₄⁺, PO₄³⁻, and silicate regeneration. Sinking POC from surface waters accounted for 50 to 100% of bottom-layer respiration in the middle estuary, with deficits partially compensated by organic carbon delivered in landward flowing bottom water. Lateral transport of POC to the central channel from adjacent shallow waters was required to meet bottom water respiratory demands. Bottom-layer regeneration and subsequent upward transport of nutrients were sufficient to support 70 to 80% of summer rates of net organic production in surface layers. Pelagic and benthic processes were most tightly linked in the middle estuary, which is highly productive and does not interact strongly with adjacent waters. Elevated nutrient inputs to the estuary associated with high freshwater flow enhanced chlorophyll *a*, net O₂ production, and net DIN uptake in surface layers; however, muted effects of flow on bottom-layer processes suggest that much of the increased organic production in surface layers during high flow is transported to seaward regions.

KEY WORDS: Estuary · Biogeochemistry · Box model · Water quality · Monitoring · Patuxent River

—Resale or republication not permitted without written consent of the publisher—

INTRODUCTION

Estuarine ecosystems form the transition zone between adjacent terrestrial, riverine, and oceanic regions. Biogeochemically reactive materials enter estuaries from the watershed and atmosphere and are processed within estuarine systems prior to being transported to the ocean (Kemp & Boynton 1984). Estuarine processing of anthropogenic and terrestrially derived materials is regulated by a balance between

physical transport and biogeochemical uptake and recycling (Kemp & Boynton 1984, Smith et al. 1991, Howarth et al. 1996). Understanding the nature and magnitude of these transformation and transport processes is essential for evaluating and managing estuarine production and nutrient cycling.

Past estuarine ecological research has elucidated regional variation in key biogeochemical processes (e.g. Cloern et al. 1983, Smith et al. 1991, Cowan et al. 1996). In upper regions of estuaries, high organic car-

*Email: jtesta@hpl.umces.edu

bon loads and high turbidity cause low phytoplankton productivity (Pennock & Sharp 1994) and net ecosystem heterotrophy (Smith et al. 1991, Heath 1995, Kemp et al. 1997). Phytoplankton biomass and productivity maxima often occur in regions with high nutrients and sufficient light (Kocum et al. 2002), typically the seaward reaches of the estuary (Harding et al. 2002). Regional maxima of benthic respiration and nutrient regeneration tend to occur in regions with the highest surface water productivity and phytoplankton biomass (e.g. Cowan & Boynton 1996).

Estuarine biogeochemical processes also exhibit distinct seasonal trends. Although peak phytoplankton biomass may occur in summer or spring, primary productivity maxima tend to occur in summer for temperate estuaries (Harding et al. 2002). Net ecosystem production (i.e. total ecosystem organic production minus respiration) also varies seasonally, depending on the magnitude and timing of freshwater, organic carbon, and inorganic nutrient inputs (Smith & Hollibaugh 1997, Kemp et al. 1997). In many temperate systems, benthic nutrient regeneration tends to follow seasonal temperature cycles (Fisher et al. 1982, Cowan & Boynton 1996).

Seasonal and regional patterns in biogeochemical processes may be mediated by horizontal and vertical transport. Under high freshwater flow conditions, elevated nutrient inputs fuel phytoplankton biomass and sinking (Boynton & Kemp 2000), but strong horizontal seaward transport may separate regions of high productivity from depositional areas (Hagy et al. 2005). Although the timing or magnitude of benthic respiration and nutrient regeneration are strongly regulated by temperature (Cowan et al. 1996), these processes often respond rapidly to vertical sinking of particulate organic material (Graf et al. 1982, Boynton & Rohland 2001). Nutrients regenerated from sinking organic material may then be transported vertically to surface waters to fuel productivity (Kemp & Boynton 1984, Malone et al. 1988).

A conceptual model was developed to describe how linkages between biogeochemical and physical processes vary seasonally and regionally in partially-stratified estuaries (Kemp & Boynton 1984). The model suggested that large spring nutrient inputs are transformed from dissolved into particulate forms in upper estuarine regions and transported seaward, where they sink to the bottom layer and are decomposed to regenerate dissolved inorganic nutrients which diffuse upward to fuel summer peaks in phytoplankton productivity. Because this hypothetical model is qualitative, it would be useful to examine these coupled ecological, biogeochemical, and physical transport processes using a quantitative, integrated approach.

The purpose of this paper is to provide such an

analysis for a partially-stratified estuary using a salt- and water-balance 'box model' applied to water quality monitoring databases to compute rates of net biogeochemical production and physical transport for nutrients, O_2 , and organic carbon. The specific objectives of this analysis were to: (1) quantify and assess the seasonal and regional coupling of nutrient delivery and transformation with organic production; (2) quantify the seasonal coupling between organic production, POC sinking, and benthic respiration; and (3) determine how variations in river flow effect biogeochemical processes.

METHODS

Study site and data availability. The Patuxent River estuary is a tributary system of Chesapeake Bay (Fig. 1). The estuary is ~65 km long, has a mean low-water estuarine volume of $577 \times 10^6 \text{ m}^3$, and a surface area of $126 \times 10^6 \text{ m}^2$. It averages 2.2 km in width and 6.0 m in depth over the most seaward 45 km of the estuary with a mean tidal range varying from 0.4 m

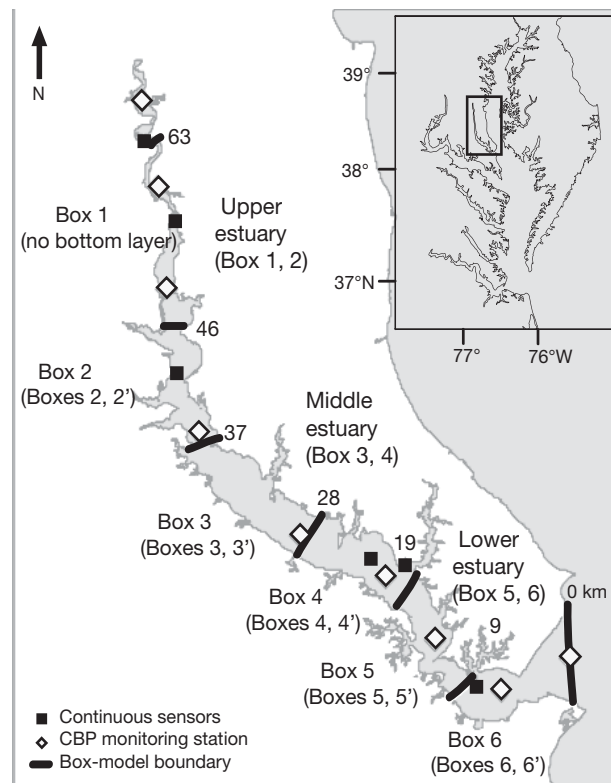


Fig. 1. Patuxent River estuary with Chesapeake Bay (inset), including box-model boundaries (Hagy et al. 2000), water quality monitoring stations, and the location of Maryland Department of Natural Resources' continuous water quality sensors. Numbers to the right of box-model boundaries indicate distance (km) from the mouth of the estuary

near the estuary mouth to 0.8 m in the upper estuary (Hagy 1996). Two-layered circulation occurs for most of the year in the estuary, with a seaward-flowing surface layer and a landward-flowing bottom layer. The upper estuary (above km 45) is vertically well-mixed. Freshwater discharge at the head of the tide averaged $10.3 \text{ m}^3 \text{ s}^{-1}$ from 1977 to 2003 (<http://va.water.usgs.gov/chesbay/RIMP/adaps2/pat.adaps.dat>). Water quality has been monitored at 2 to 4 wk intervals for 9 stations along the estuarine axis since 1985, including measurements of salinity, temperature, O_2 , chlorophyll *a* (chl *a*), and dissolved and particulate forms of nutrients and organic carbon (www.chesapeakebay.net, Fig. 1). In addition, a series of continuous water quality sensors (measuring O_2 , temperature, chl *a*) were deployed from spring through fall at 6 stations in the estuary (www.eyesonthebay.net, www.act-us.info).

Computing salt and water transport. In this study, we computed the Patuxent estuary's time-dependent, seasonal mean circulation using mean monthly salinity (www.chesapeakebay.net) and freshwater input data (<http://va.water.usgs.gov/chesbay/RIMP/adaps2/pat.adaps.dat>, <http://www7.ncdc.noaa.gov/IPM/MCDWPPubs?action=getpublication>). This box-modeling approach computes advective and diffusive exchanges of water and salt between adjacent control volumes (which are assumed to be well-mixed) and across end-member boundaries using the solution to non-steady-state equations balancing salt and water inputs, outputs, and storage changes (Pritchard 1969, Officer 1980, Hagy et al. 2000). Stratified estuarine regions are represented by surface and bottom layers that capture the essential features of 2-layered estuarine circulation (Pritchard 1969). The box model used in this analysis calculates advection and mixing between 6 boxes in the Patuxent River estuary (Boxes 2 to 6 include surface and bottom-layer sub-boxes, Figs. 1 & 2; Hagy et al. 2000). Boundaries separating adjacent boxes were defined based on data availability, degree of density stratification, and an effort to retain similar salinity gradients and water volumes among boxes. The salt and water balances (Eqs. 1 & 2 respectively) for a surface-layer box '*m*' in the 2-layer scheme are described below:

$$V_m \frac{ds_m}{dt} = Q_{m-1}s_{m-1} + Q_{vm}s'_m - Q_m s_m + E_{vm}(s'_m - s_m) + E_{m-1,m}(s_{m-1} - s_m) + E_{m,m+1}(s_{m+1} - s_m) \quad (1)$$

$$\frac{dV_m}{dt} = 0 = Q_m - (Q_{m-1} + Q_{vm} + Q_{im}) \quad (2)$$

where V_m is the volume of the box, Q_m and Q_{m-1} are the advective transports to the seaward box and from the landward box, Q_{vm} is the vertical advective input into the box, $E_{m-1,m}$ and $E_{m,m+1}$ are the diffusive

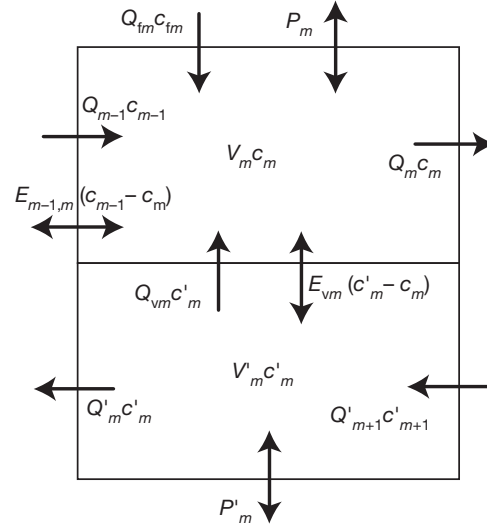


Fig. 2. Two-layer non-conservative box model for Boxes 2–6. Arrows represent advective (Q), non-advective (E), and net production (P) terms for the box. The non-advective exchange, $E_{m,m-1}(c_m - c_{m-1})$, is a term for the calculation in the surface layer of Box 2 only. Atmospheric inputs are included ($Q_{im}c_{im}$) for the non-conservative DIN flux. Refer to Hagy et al. (2000) for further details

exchanges with the landward and seaward boxes, E_{vm} is the vertical diffusive exchange, s_m and s'_m are the salinities in the upper and bottom-layer boxes, and s_{m-1} and s_{m+1} are the salinities in the landward and seaward boxes, and t is time. We assumed that $E_{m,m-1} = 0$ for $m \neq 2$, $E_{m,m+1} = 0$ for $m \neq 1$, and $E_{vm} = 0$ and $Q_{vm} = 0$ for $m = 1$ (Officer 1980, Hagy et al. 2000). For Eq. (2), Q_{im} is the freshwater input directly into the box. The left hand side of Eq. (1) is computed as the monthly salinity change, while the left hand side of Eq. (2) is assumed to be zero at monthly time scales. The salt and water balances (Eqs. 3 & 4) for a bottom-layer box '*m*' in the 2-dimensional scheme are similar:

$$V'_m \frac{ds'_m}{dt} = Q'_{m+1}s'_{m+1} - Q'_{vm}s'_m - Q'_m s'_m - E_{vm}(s'_m - s_m) \quad (3)$$

$$\frac{dV'_m}{dt} = 0 = Q'_m + Q'_{vm} - Q'_{m+1} \quad (4)$$

where Q'_m and Q'_{m+1} are the advective transports to the landward box and from the seaward box and s'_{m+1} is the salinity of the seaward box in the bottom layer.

Nutrient transport and production rates. We computed monthly and seasonal rates of transport and net biogeochemical production of dissolved O_2 , nutrients, and organic carbon for 6 regions of the Patuxent River estuary from 1985 to 2003. Physical transport rates for these non-conservative biogeochemical variables were computed by multiplying the solute concentration by the advective and non-advective fluxes (Q 's and E 's,

respectively) for each box and month. Rates were calculated for the following variables: (1) dissolved inorganic nitrogen ($\text{DIN} = \text{NO}_2^- + \text{NO}_3^- + \text{NH}_4^+$), (2) dissolved inorganic phosphorus ($\text{DIP} = \text{PO}_4^{3-}$), (3) dissolved silicate (DSi), (4) total organic carbon (TOC), and (5) dissolved O_2 . Monthly mean values of these variables were computed for each box (and upstream and downstream boundaries) from water quality monitoring data (see Fig. 1 for monitoring stations) using a simple linear spatial interpolation scheme with a grid of 477 cells spaced at 1 m vertical intervals, 1.85 km horizontal intervals, and spanning the width of the estuary for each sampling date (Hagy et al. 2000). Net biogeochemical production rates (P_m or $P'_m = \text{production} - \text{consumption}$) for each non-conservative water quality variable were computed for each box using the analytical solutions for the advective (Q) and diffusive (E) transport rates in each box. The equations are similar in form to Eqs. (1) & (2), except salinity is replaced with the water quality variable and the net production term (P_m or P'_m) is added. Thus, for a surface-layer box ' m ' in the 2-layer scheme of the box-model without longitudinal E 's, the mass balance equation is:

$$V_m \frac{dc_m}{dt} = Q_{m-1}c_{m-1} + Q_{vm}c'_m + E_{vm}(c'_m - c_m) - Q_m c_m + P_m \quad (5)$$

which can be rearranged to calculate P_m :

$$P_m = V_m \frac{dc_m}{dt} - Q_{m-1}c_{m-1} - Q_{vm}c'_m - E_{vm}(c'_m - c_m) + Q_m c_m \quad (6)$$

For any bottom-layer box ' m ', the mass balance expression is:

$$V'_m \frac{dc'_m}{dt} = Q'_{m+1}c'_{m+1} - Q_{vm}c'_m - Q'_m c'_m - E_{vm}(c'_m - c_m) + P'_m \quad (7)$$

which can be rearranged to calculate bottom-layer net production, P'_m :

$$P'_m = V'_m \frac{dc'_m}{dt} - Q'_{m+1}c'_{m+1} + Q_{vm}c'_m + Q'_m c'_m + E_{vm}(c'_m - c_m) \quad (8)$$

where c is the concentration of the non-conservative material and P_m and P'_m are the net production (or consumption) rates in the surface and bottom layers, calculated per unit area or volume using geometry data for each box (Table 1).

Input terms for wet atmospheric deposition of DIN were added to mass-balance equations of surface-layer boxes and deposition rates were calculated using data for precipitation volume and concentrations of NO_3^- and NH_4^+ (<http://nadp.sws.uiuc.edu>). We also

Table 1. Physical dimensions of all boxes for the box model of Hagy et al. (2000). Dimension information may be used to convert all box model computed nutrient transport and production rates to the desired units. MLW: area of each surface box at mean low water. Box boundaries are shown in Fig. 1

Box	Volume (10^6 m^3)		Surface area (10^6 m^2)		Mean depth (m)	
	Surface	Bottom	MLW	Pycnocline	Surface	Bottom
1	17.60		7.20		2.43	
2	29.70	3.50	17.90	1.70	1.66	2.03
3	63.80	17.90	26.10	5.90	2.45	3.03
4	104.00	33.50	28.40	7.30	3.67	4.57
5	110.00	44.00	24.20	5.80	4.53	7.59
6	100.00	62.80	22.20	9.00	4.50	6.95

tested for the effects of direct non-point nutrient inputs to each box using the Chesapeake Bay Watershed Model (Linker et al. 1996, L. Linker pers. comm.) and found that these terms did not substantially affect the net production rates. We omitted non-point inputs in our calculations due to widely recognized uncertainties in model-generated loading rates and to prevent the introduction of unknown error (Williams et al. 2006).

Computing net production of dissolved O_2 in surface layers required adjustments to O_2 concentrations and the box-model calculation. The first step was to adjust observed O_2 concentrations at a particular time of day to the equivalent daily mean O_2 value for that day. This was accomplished using measurements of diel variations in O_2 concentrations (15 min intervals) observed at nearby moored-sensor stations (Fig. 1). Hourly mean O_2 values (as % saturation) were calculated for each month of the year at 6 moored-sensor stations (www.eyesonthebay.net, www.act-us.info, Fig. 1) that span the estuarine axis; for the 2 surface boxes without a sensor, we used the average of the 2 adjacent boxes. We then calculated a 'diel correction' coefficient for each hour of the day in each month at each station as the ratio of the daily mean O_2 concentration to the hourly mean O_2 concentration for the sampling hour in that day. The 'daily mean corrected' O_2 value was calculated by multiplying the measured O_2 concentration from the grab sample by the 'diel correction' coefficient for time of day and month.

The second step involved adjusting computed rates of net O_2 production in surface boxes for the effects of air-water gas exchange. We computed the air-water O_2 exchange ($F_{A-\text{O}_2}$) on monthly time-scales using O_2 values measured in the top 0.5 m of the water column (corrected for time of day) following Caffrey (2003): $F_{A-\text{O}_2} = \alpha(1 - C_{\text{O}_2}/C_{\text{O}_2s})$ where α is the air-water exchange coefficient ($\text{mmol O}_2 \text{ m}^{-2} \text{ d}^{-1}$), C_{O_2} is the adjusted daily mean O_2 concentration at 0.5 m depth (mmol m^{-3}), and C_{O_2s} is the O_2 saturation value (mmol

m^{-3}). Using published relationships with wind speed (e.g. Marino & Howarth 1993) and monthly mean wind data observed at the nearby airport, we chose a value for α of $3.75 \times 10^2 \text{ mmol m}^{-2} \text{ d}^{-1}$ ($0.5 \text{ g m}^{-2} \text{ h}^{-1}$) for all months. Analyses of wind data suggested that there were significant variations in wind velocity on daily to weekly scales, but there were no significant monthly or seasonal trends.

Assessing error in box-model rates. The monitoring data used to compute monthly mean concentrations for a given control volume in each box were collected from vertical profiles at mid-channel stations (Fig. 1) at 2 to 4 wk intervals. Although the boxes span the width of the estuary, containing both deep 2-layer regions near the estuarine channel and shallow (<4 m) vertically mixed areas flanking the channel, previous studies of Chesapeake Bay tributary monitoring data revealed that parallel measurements at mid-channel and adjacent near-shore areas were statistically indistinguishable for 90% of the time when stations were <2 km apart (Kemp et al. 2004). Comparisons of continuous (15 min) mid-channel measurements of salinity and O_2 (www.act-us.info) with measurements from shallow water sensors in 2004 (www.eyesonthebay.net) showed significant correlations between the 2 sites (salinity: $r^2 = 0.50$, O_2 : $r^2 = 0.43$, $p < 0.01$) and nearly equivalent means. In addition, significant correlations between monthly averages of mid-channel grab samples (www.chesapeakebay.net) and continuous shallow water sensors in 2004 and 2005 suggest that mid-channel grab samples characterize the key temporal variability for entire boxes (salinity: $r^2 = 0.91$ – 0.98 , O_2 : $r^2 = 0.72$ – 0.95 , $p < 0.01$). Slopes of the linear fits were always ~ 1 (range: 0.75–1.4).

Stoichiometric calculations. The net production rates computed with the box-model were used to estimate additional biogeochemical processes by assuming fixed stoichiometric relationships between variables ($\text{C}:\text{Si}:\text{O}_2$) based on elemental compositions of algal (e.g. diatom) cells (Redfield 1958). We estimated the contribution of diatom photosynthesis to total net organic carbon production rates by applying a stoichiometric adjustment to the computed surface-layer net DSi production rate: $P_{\text{C}}\text{Si}_m = k_{\text{C}:\text{Si}}(-P\text{Si}_m)$, where $P_{\text{C}}\text{Si}_m$ is the net carbon production (for Box m) attributed to diatoms ($\text{mmol C m}^{-3} \text{ d}^{-1}$), $k_{\text{C}:\text{Si}}$ is the assumed carbon-silica ratio for diatoms of 6.625 (Redfield 1958), and $P\text{Si}_m$ is the computed surface net DSi production rate ($\text{mmol Si m}^{-3} \text{ d}^{-1}$) for Box m (Hagy 1996).

We also estimated the sinking flux of particulate organic carbon, POC ($S_{\text{POC}m}$, $\text{mmol C m}^{-2} \text{ d}^{-1}$) between surface and bottom layers using box-model computed net production rates for O_2 and total organic carbon (TOC) in the surface layer in the stratified estuarine regions (Boxes 2–6) as follows: $S_{\text{POC}m} = k_{\text{C}:\text{O}} P\text{O}_{2m} -$

$P_{\text{TOC}m}$, where $P\text{O}_{2m}$ is the surface-layer net O_2 production rate ($\text{mmol O}_2 \text{ m}^{-2} \text{ d}^{-1}$), $P_{\text{TOC}m}$ is surface-layer net production rate of TOC ($\text{mmol C m}^{-2} \text{ d}^{-1}$), and $k_{\text{C}:\text{O}}$ is the photosynthetic quotient (assumed to be 1.0). This formulation assumes that, in the absence of POC sinking, net O_2 production (converted to carbon units) and TOC production are equivalent.

RESULTS

Spatial and temporal variation in concentrations

Typical seasonal and regional variations in concentration and distribution of chl a , salinity, and dissolved O_2 are illustrated using time-space isopleths for 1995, a year of average freshwater flow (Fig. 3). A phytoplankton chl a peak occurred in early spring during the period of maximum nutrient loading (Kemp and Boynton 1984) and migrated seaward during the following month, eventually disappearing from the water column in late spring (Fig. 3). The peak extended to 7 to 10 m in depth and 20 to 30 km along the axis of the middle estuary (Fig. 3). There was a vertical gradient in chl a , with the higher concentrations in the surface in early spring, but in the bottom during late spring. Hypoxia ($\text{O}_2 < 2 \text{ mg l}^{-1}$) developed in deep water during late spring (May to June) in the region where the chl a peak occurred earlier in the season (February to April; Fig. 3). Nutrient concentrations were generally highest in the upper estuary. Seasonal minima of DIN and DSi occurred in the middle and lower estuary during summer, while DIP peaked during summer in these regions.

Seasonal variation in modeled non-conservative rates

Rates of net biogeochemical production for non-conservative water quality variables were computed for each month over the 19 yr record and monthly mean values (\pm SE) were computed for all years. Strong seasonal trends were evident in the data. Monthly box-model-computed net production rates for all years in the data set (19 yr) were grouped ($n = 12$) and a 1-way ANOVA with a Scheffe's Test was used to determine if the monthly rates were significantly different in each estuarine region. These tests revealed that the peak seasonal rates were significantly ($p < 0.05$) higher than seasonal minimum rates for all variables, except for surface-layer net O_2 production in the middle and lower estuary.

In the upper estuary, peaks in net O_2 uptake ($-80 \text{ mmol O}_2 \text{ m}^{-2} \text{ d}^{-1}$) corresponded to peaks in net DIP production in summer, but with reduced net DIN

and DSi uptake ($<2 \text{ mmol m}^{-2} \text{ d}^{-1}$) relative to other regions (Fig. 4). Surface net O_2 production (net autotrophy) peaked in late spring (60 to $80 \text{ mmol m}^{-2} \text{ d}^{-1}$) in the middle and lower estuary and was linked to net DSi uptake ($-5 \text{ mmol Si m}^{-2} \text{ d}^{-1}$) and the seasonal

chl *a* peak (see Fig. 8). In summer, however, there was net production (10 to $25 \text{ mmol Si m}^{-2} \text{ d}^{-1}$) of DSi throughout the estuary. The annual peak in net DIN uptake ($-5 \text{ mmol N m}^{-2} \text{ d}^{-1}$) lagged ~ 1 mo behind the maximum of net O_2 production.

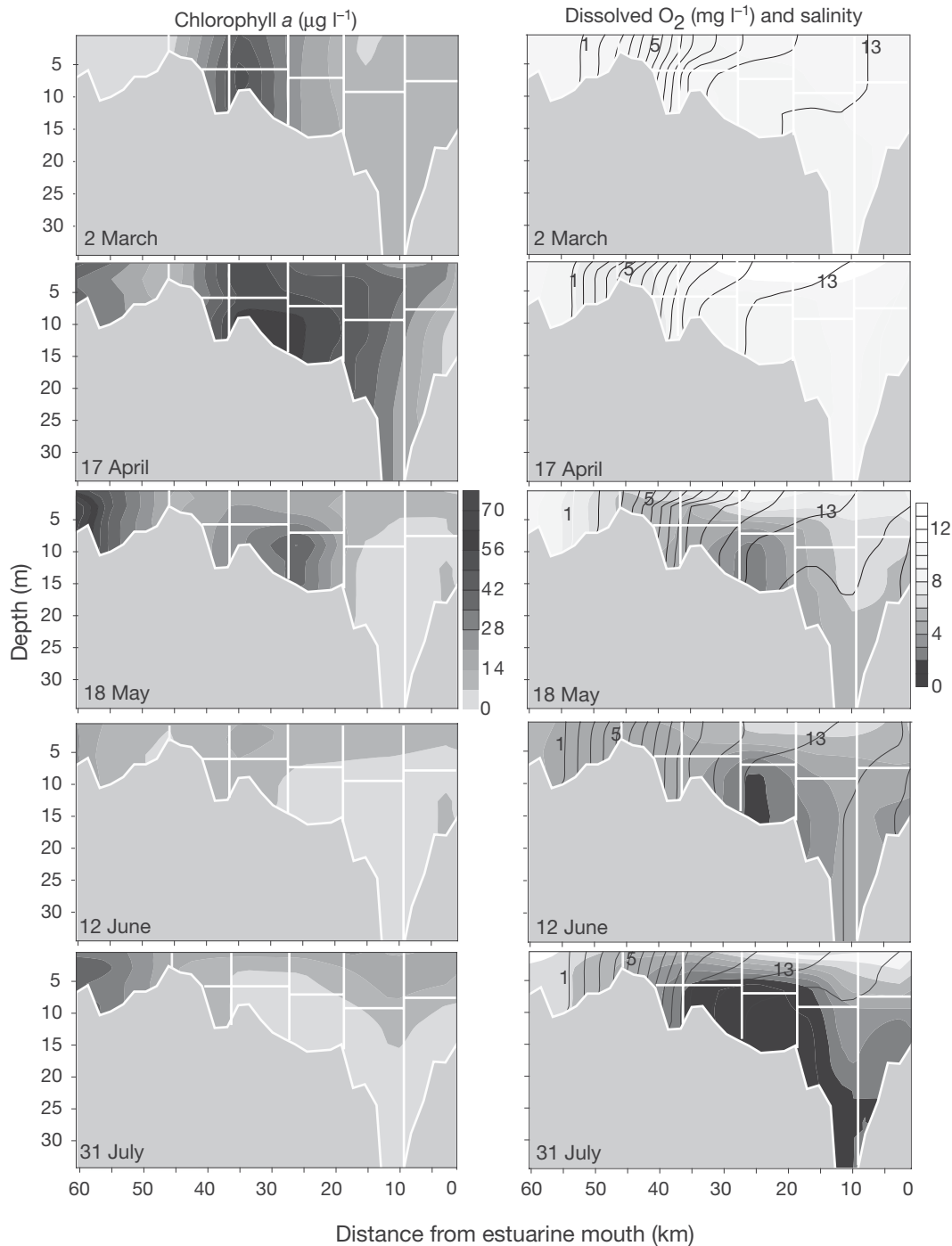


Fig. 3. Contour plots of water quality monitoring data for chl *a* (left-hand panels) and dissolved oxygen/salinity (right-hand panels) in the Patuxent River estuary in the winter, spring, and summer of 1995. White lines: box-model boundaries. O_2 /salinity graphs — numbers are salinity-contour values; black areas: hypoxic water ($\text{O}_2 < 2 \text{ mg l}^{-1}$). Data acquired from www.chesapeakebay.net

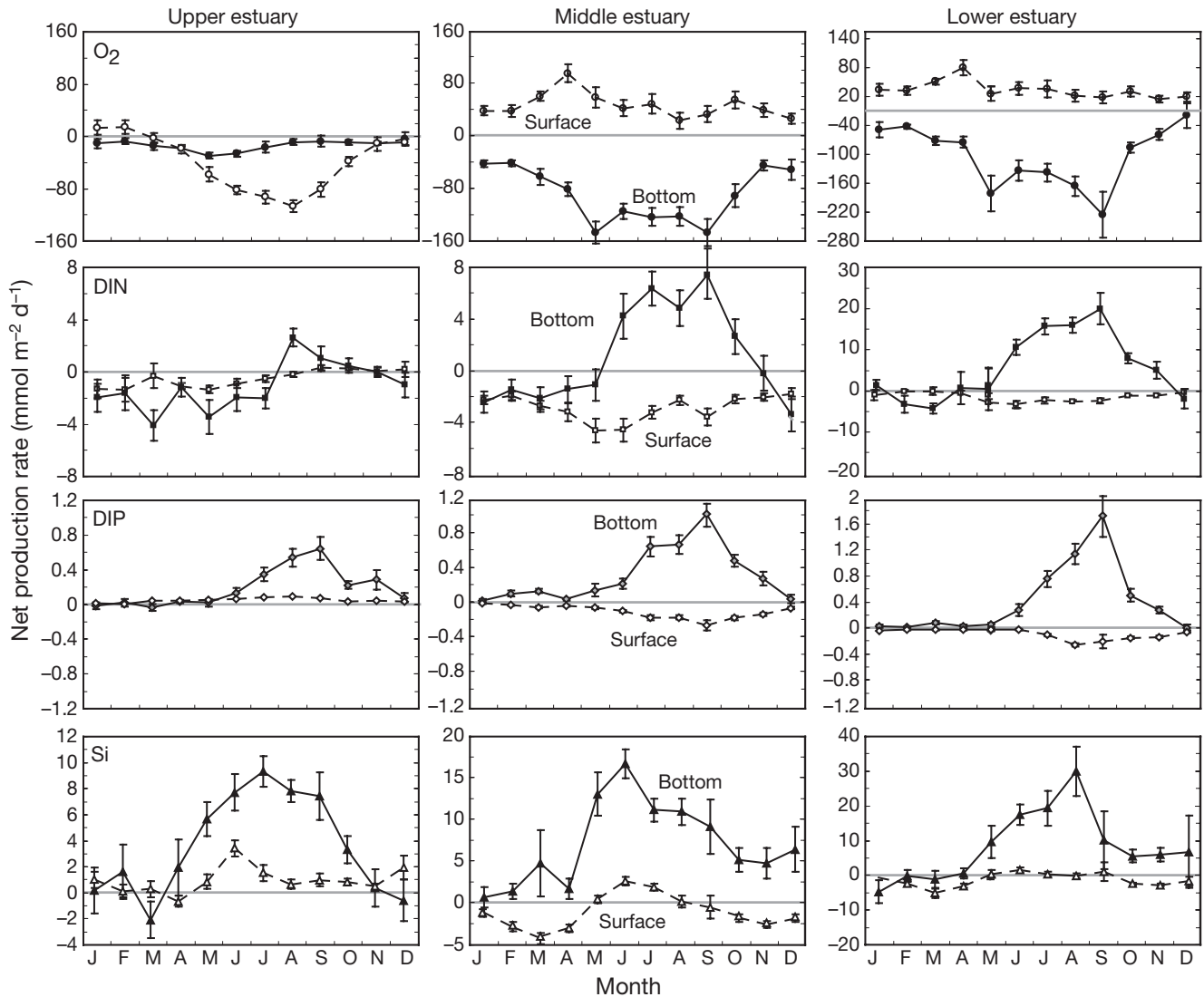


Fig. 4. Monthly mean (\pm SE) net biogeochemical production rates (1985–2003) of (---) surface and (—) bottom-layer O_2 (surface rate corrected for air–water exchange), DIN, DIP, and DSi, computed by the box-model for the upper (Box 2), middle (Box 4), and lower (Box 5) Patuxent River estuary

Bottom-layer rates of net DSi (8 to 20 $mmol Si m^{-2} d^{-1}$), DIN (4 to 20 $mmol N m^{-2} d^{-1}$), and DIP (0.6 to 1.2 $mmol P m^{-2} d^{-1}$) production peaked between May and September throughout the estuary corresponding to peaks in net O_2 uptake (Fig. 4). DIP, NH_4^+ , and DSi regeneration and bottom net O_2 uptake were significantly correlated with temperature throughout the estuary, but the correlations were highest in the middle estuary (Fig. 5). The magnitudes of nutrient regeneration and O_2 uptake m^{-2} were generally highest in the lower estuary (see Fig. 7). Despite these relationships, 50 to 80% of the variation was not explained by temperature.

On a monthly scale, surface-layer rates of net O_2 production and net nutrient uptake were generally en-

hanced in wet years (river flow > 20 yr average), relative to dry years (Fig. 6; net O_2 production was elevated by 1 to 15 $mmol m^{-2} d^{-1}$). In the surface layers of the middle and lower estuary during the summer of wet years, measured chl *a* levels were elevated by 10 to 15 $\mu g l^{-1}$. Consequently, summer net DIN uptake was 0.3 to 1.5 $mmol m^{-3} d^{-1}$ higher during wet years and the summer peak persisted later in the year in the middle and lower estuary. Differences between surface-layer net O_2 production, net DIN uptake, and measured chl *a* in the summers (averaged over May–August) of wet versus dry years were significant in the middle and lower estuary, but bottom-layer rates were not significantly affected by flow (ANOVA, $p < 0.05$).

Axial distributions of modeled non-conservative rates

Surface-layer rates of net O_2 production reveal a gradient along the estuary's length from net heterotrophy in landward estuarine regions to net autotrophy in seaward regions (Boxes 1 & 2 and 3 to 5 respectively), with peak net O_2 production (40 to 100 $mmol O_2 m^{-2} d^{-1}$) occurring in the middle estuary (Fig. 7). Axial chl *a* dis-

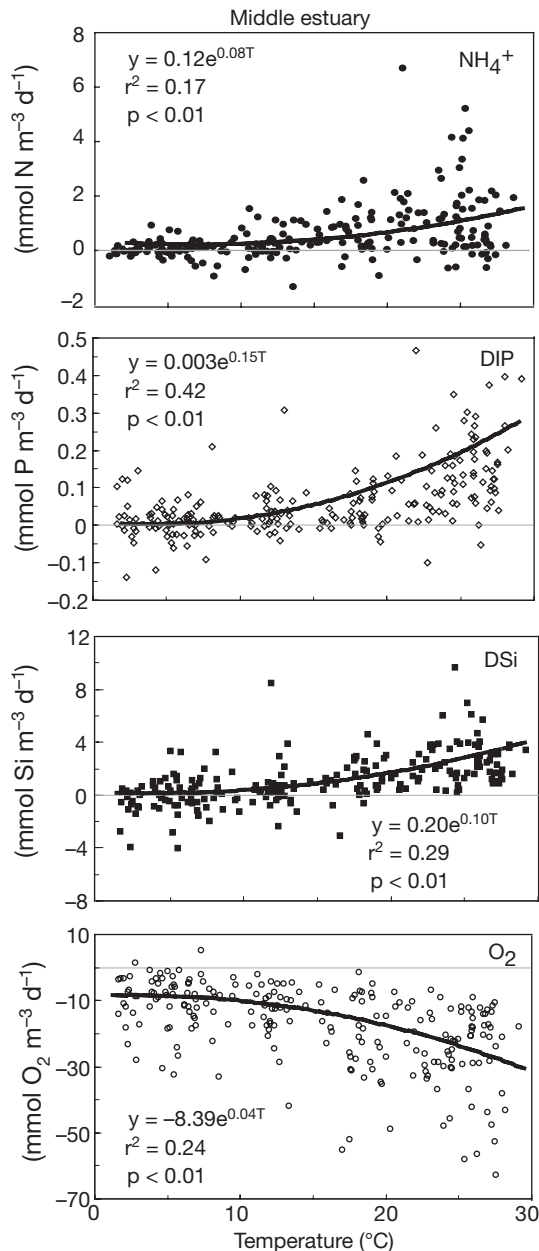


Fig. 5. Relationships between temperature and monthly rates of net bottom-layer production of NH_4^+ , DIP, DSi, and O_2 , computed by the box-model for the middle (Box 4) Patuxent River estuary

tributions revealed a peak in Boxes 3 & 4, where the highest net O_2 production rates occurred. The highest chl *a* measurements were made during spring in the middle and lower estuary (spring bloom) and in summer in the upper estuary (Boxes 1 & 2). Net DIN and DIP uptake occurred in the surface layer of Boxes 3 to 6, and highest rates (0.08 to 0.16 $mmol DIP m^{-2} d^{-1}$, 3 to 4 $mmol DIN m^{-2} d^{-1}$) occurred in the middle estuary, where net O_2 production rates and chl *a* were highest.

On the annual scale, net O_2 production was nearly twice as high during wet years than during dry years, but bottom-layer net O_2 uptake did not significantly increase with higher flow (Fig. 7). Chl *a* was significantly ($p < 0.01$) elevated and the regional peak shifted 20 km seaward under high flow conditions. Surface-layer rates of net DIN and DIP uptake were highest in the middle estuary during wet years and increased with river flow up to 30%. Mean annual rates of river flow were positively correlated with mean annual chl *a* ($r^2 = 0.24$ to 0.50, $p < 0.01$), net DIN uptake ($r^2 = 0.32$ –0.46, $p < 0.01$), and net O_2 uptake ($r^2 = 0.38$ to 0.56, $p < 0.01$) in the middle and lower estuary. During wet years, surface net DIP uptake increased in the middle estuary (Boxes 2 to 5), but decreased at the landward and seaward extremes (Boxes 1 & 6 respectively). Bottom-layer net O_2 uptake, chl *a*, and DIP production were 5 to 30% higher in wet years relative to dry years in the middle and lower estuary, but these differences were not significant ($p > 0.05$, Fig. 7). The axial distribution of rate magnitudes did not change with variation in freshwater inputs.

Stoichiometric computations

Seasonal patterns of POC sinking generally followed those observed for POC concentration and peaked at 75 to 100 $mmol C m^{-2} d^{-1}$ in late winter and spring (February to April) throughout the estuary (Fig. 8). A spring peak in net DSi uptake (5 $mmol C m^{-3} d^{-1}$) occurred in the middle estuary (Boxes 3 & 4; Fig. 8). POC sinking and concentration and chl *a* were higher in the middle estuary than lower regions. POC sinking rates were relatively low during summer, but increased to a fall peak of 10 to 30 $mmol C m^{-2} d^{-1}$. Computed settling rates (calculated as POC sinking flux divided by the POC concentration) ranged from 0.4 to 0.6 $m d^{-1}$ during winter spring and 0.1 to 0.2 $m d^{-1}$ during summer.

Pelagic-benthic coupling

Relationships between surface- and bottom-layer biogeochemical rates illustrate the nature and regional

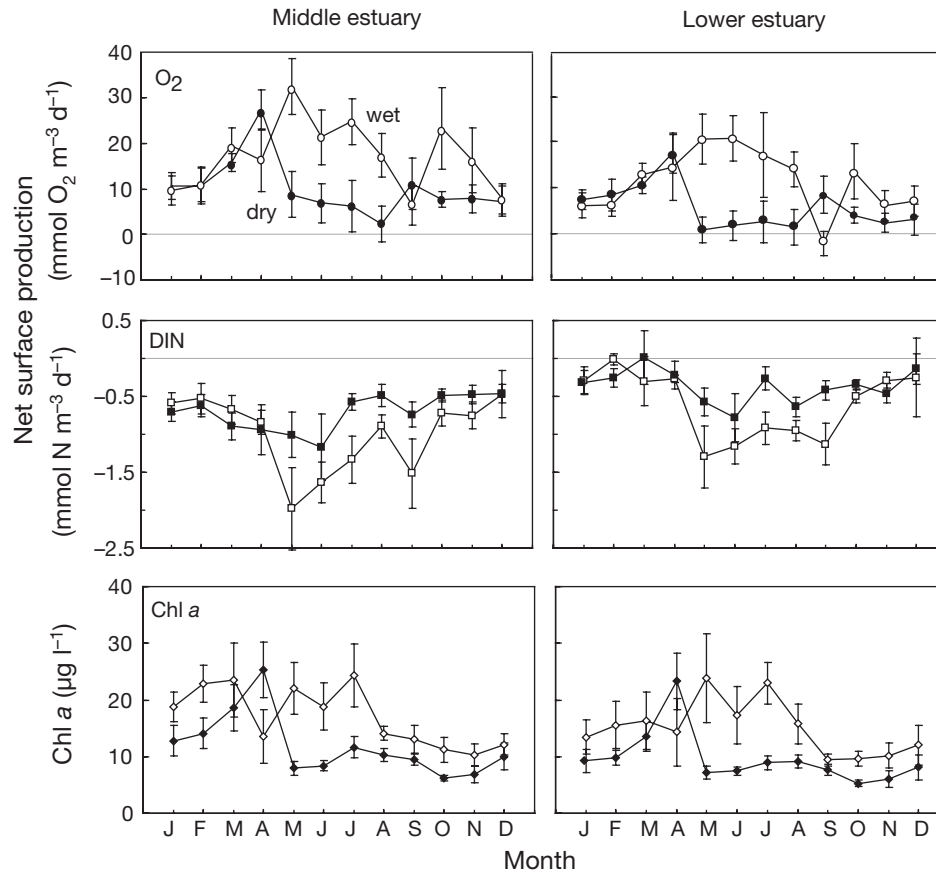


Fig. 6. Monthly mean net biogeochemical production rates of O_2 (corrected for air–water exchange) and DIN, computed for the surface layer by the box-model, as well as chl *a*, in the surface layer of the middle (Box 4) and lower (Box 5) Patuxent River estuary. Monthly means (\pm SE) were calculated for years of above-average (open) (flow > 20-yr mean, $n = 7$) and below-average river flow (filled) (flow < 20-yr mean, $n = 9$)

variations of vertical coupling along the estuarine axis. We found significant ($p < 0.05$) positive correlations between modeled annual mean surface-layer net O_2 production and bottom-layer O_2 uptake in the middle ($r^2 = 0.43$, $p < 0.01$, Fig. 9a) and lower estuary ($r^2 = 0.26$, $p < 0.05$). The correlation was strongest and the rates were highest in the middle estuary with reduced rates in the lower estuary. Modeled surface-layer net O_2 production (0.3 to 1.3×10^3 kmol O_2 d^{-1}) exceeded bottom-layer net O_2 uptake (0.3 to 0.9×10^3 kmol O_2 d^{-1}) in the middle estuary (Fig. 9a).

Positive correlations were observed between surface chl *a* and modeled bottom-layer net O_2 uptake and the chl *a* versus net O_2 uptake relationship was strongest for the middle estuary ($r^2 = 0.40$, $p < 0.01$) but the relationship was also significant for the upper estuary. Modeled spring POC sinking was also positively correlated with modeled bottom-layer net O_2 uptake on an annual scale in the middle estuary (Fig. 9b), but not on monthly scales. Similarly, chl *a* was significantly and positively correlated with box-model computed POC

sinking in the middle estuary. POC sinking during February to April was significantly correlated with modeled bottom-layer net NH_4^+ , DIP, and DSi production in the middle estuary (NH_4^+ : $r^2 = 0.25$, $p < 0.05$; DSi: $r^2 = 0.32$, $p < 0.05$; DIP: $r^2 = 0.51$, $p < 0.01$). Modeled bottom-layer net O_2 uptake was positively correlated with modeled NH_4^+ ($r^2 = 0.39$, $p < 0.01$) and DIP ($r^2 = 0.23$, $p < 0.05$) regeneration in the lower estuary, but significant relationships existed in the middle and lower estuary for NH_4^+ , DIP, and DSi.

Nutrient transport rates

Box-model computed DIN inputs to the upper estuary were dominated by spring seaward transports and the magnitude of seaward DIN inputs increased in more seaward boxes. The magnitude of vertical transport of DIN to upper (Box 2) and lower (Box 5) estuary surface layers was similar to seaward advection from May to October (upper: 3 mmol N m^{-2} d^{-1} ; lower:

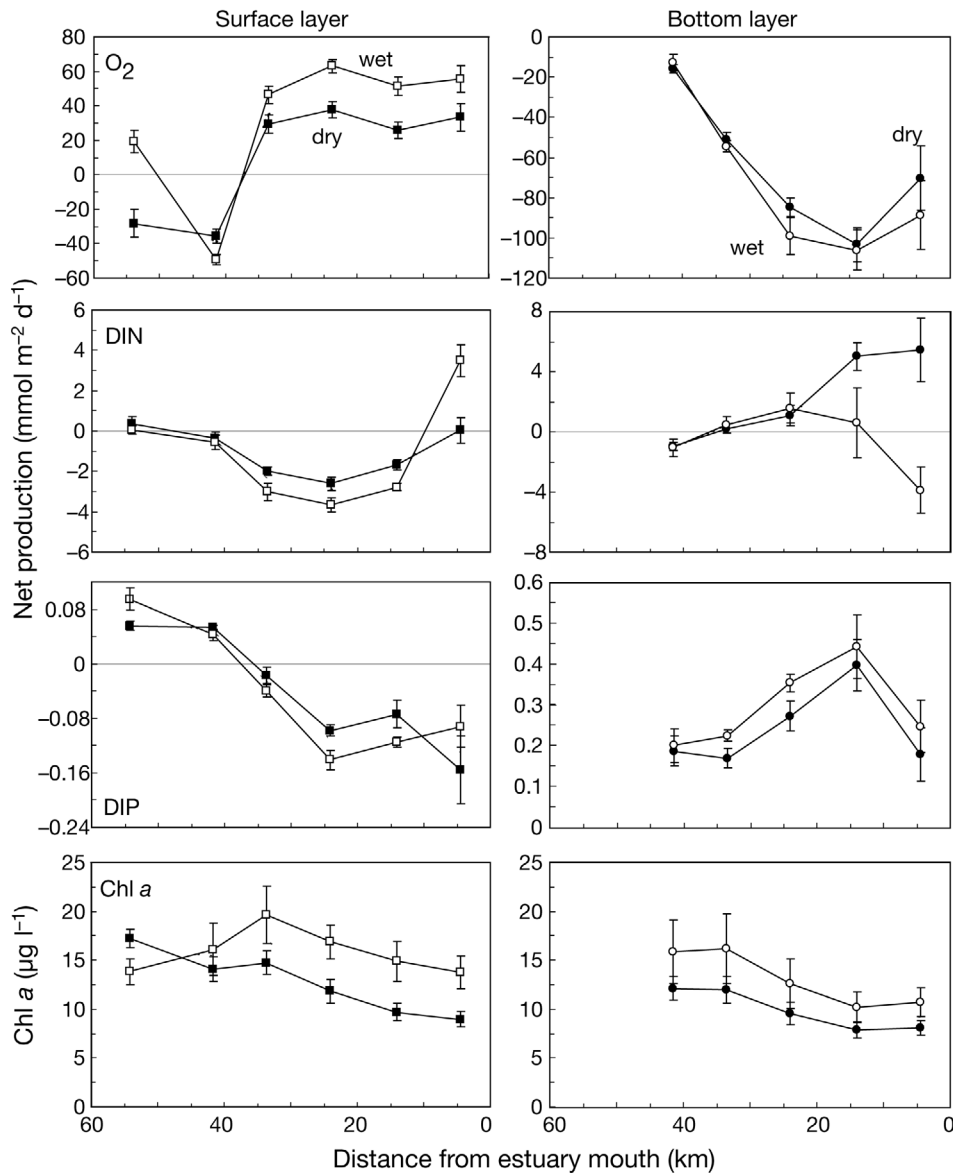


Fig. 7. Mean annual net biogeochemical production rates of surface- and bottom-layer O_2 (surface rate corrected for air–water exchange), DIN, and DIP, computed by the box-model, as well as chl *a*, along the estuarine axis of the Patuxent River estuary. Annual means (\pm SE) were calculated for years of above-average (open) and below-average (filled) river flow

$5 \text{ mmol N m}^{-2} \text{ d}^{-1}$; Fig 10b). Conversely, DIN inputs to the middle estuary (Boxes 3 & 4) were dominated by seaward advection in spring, but vertical transport dominated from May to October and was 50% higher than seaward inputs in the middle estuary (Fig. 10a). Spring DIN inputs from seaward advection were sufficient to support modeled spring net O_2 production, but vertical DIN inputs were required to support summer rates of net O_2 production in the middle estuary (Fig. 10a).

DISCUSSION

This analysis demonstrates the use of box-models to calculate integrated rates of physical transport and biogeochemical transformation of nutrients, O_2 , and organic matter using easily accessible data from a water quality monitoring program. The quantification of these rates allowed us to assess for the Patuxent River estuary the relative importance of physical transport and vertical exchange in support of biogeochemi-

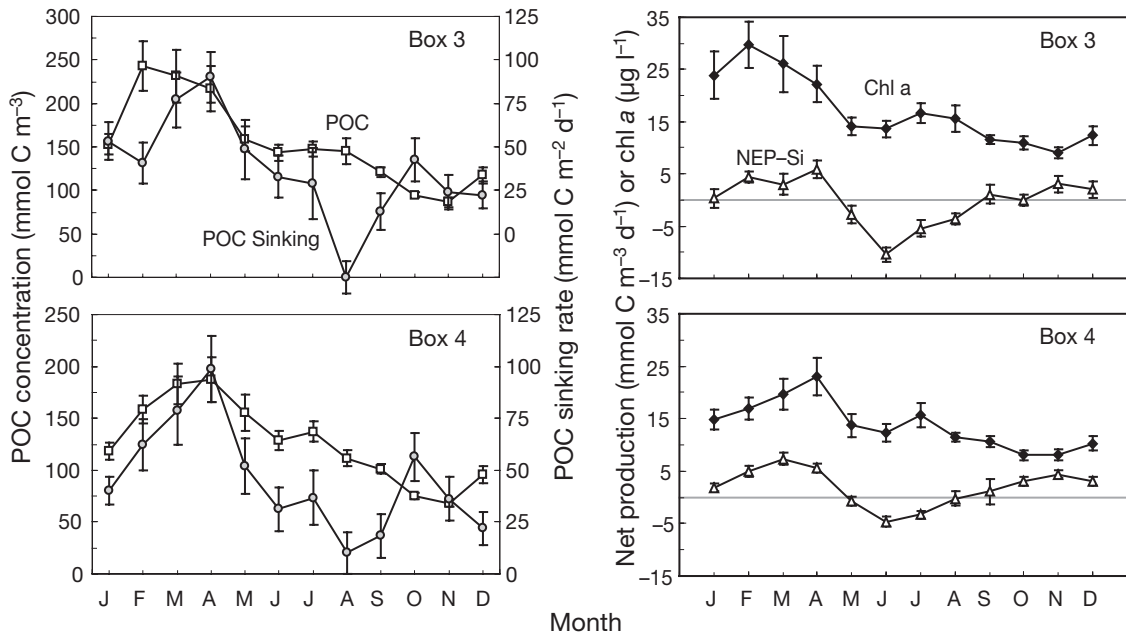


Fig. 8. Mean monthly surface-layer particulate organic carbon (POC) concentration and box-model computed POC sinking (left panels), and surface-layer net diatom growth (right panels) and net surface-layer chl a in the middle Patuxent River estuary (Boxes 3 & 4). Monthly means (\pm SE) were calculated from 1985–2003 data

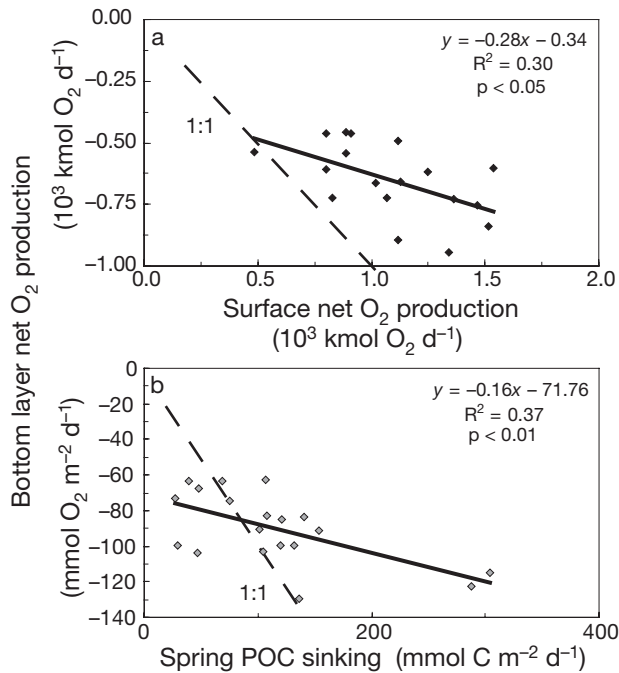


Fig. 9. Correlations of mean annual rates (1985–2003) of box-model computed net bottom-layer O₂ uptake with modeled (a) surface net O₂ production (corrected for air-water exchange) and (b) spring POC sinking (Feb–May) in the middle estuary

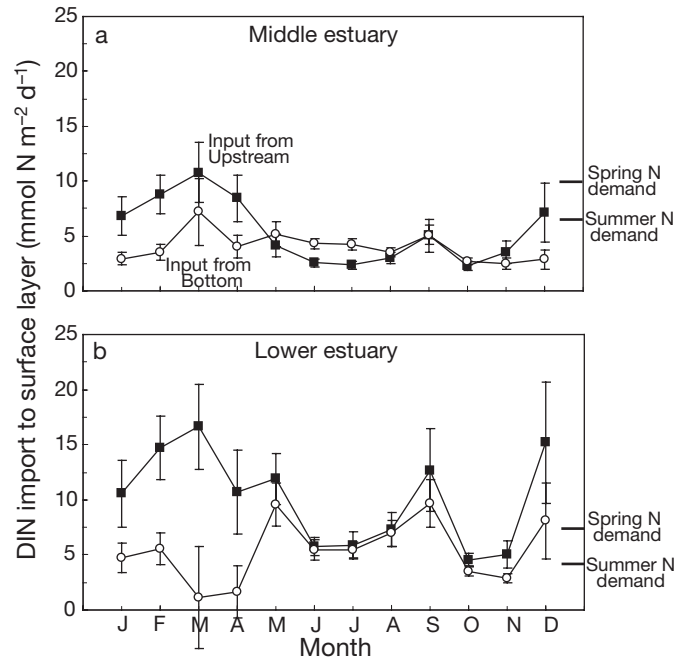


Fig. 10. Monthly mean box-model computed total inputs of DIN (\pm SE) from seaward sources (■) and vertical inputs from the bottom layer (○) to the (a) middle and (b) lower regions of the Patuxent River estuary. Summer and spring N demand was based upon modeled net O₂ production in the middle and lower estuary

cal processes, and to establish clear regional- and seasonal-scale patterns and interannual responses to climatic variation. These rates are useful for addressing a wide range of scientific questions; here, we provide 8 specific examples.

Seasonal and regional patterns in modeled surface productivity and nutrient uptake

The calculated transition from net heterotrophy in landward regions of the Patuxent to autotrophy (i.e. net carbon production) in seaward areas (Fig. 7) is a general pattern in many temperate estuaries (e.g. Heath 1995, Kemp et al. 1997), is consistent with the 'river continuum' concept (Vannote et al. 1980), and suggests that most of the organic production occurs in the mid-to-lower estuary. Net heterotrophy in the upper estuary results from both high turbidity (mean total suspended solids [TSS] = 70 mg l⁻¹, Secchi = 0.4 to 0.6 m) that limits photosynthesis (Cloern et al. 1983) and large inputs of allochthonous carbon (annual mean = 125 mmol C m⁻² d⁻¹) that fuel respiration (Smith & Hollibaugh 1997), consistent with other estuarine systems (Howarth et al. 1996). Modeled net O₂ production in seaward regions occurs where light and nutrients are abundant and allochthonous inputs are reduced relative to landward regions.

Although phytoplankton production tends to peak in mid-summer in the Patuxent (Kemp & Boynton 1984) and other coastal systems (Radach et al. 1990, Harding et al. 2002), we found that modeled net O₂ production generally exhibited seasonal maxima in late spring (e.g. Hoppema 1991). The decline of modeled net O₂ production in summer was due to increased respiration, which led to more balance between gross production and respiration (Smith & Kemp 1995). As expected, the spring net O₂ production maximum coincided with the spring diatom bloom (Malone et al. 1988) and the seasonal peak in plankton biomass. This is also consistent with the fact that regional maxima for modeled net O₂ production, nutrient uptake, and chl *a* all coincide in the middle and lower Patuxent estuary (Figs. 4 & 7).

This spatial and seasonal peak in modeled net O₂ production appears to be linked to the annual DSi cycle. Computed rates of net DSi uptake can be generally attributed to diatom growth in the Patuxent because DSi is not affected by chemical and physical reactions at typical spring concentrations (Kamatani & Riley 1979) or temperatures (<13°C, Yamada & D'Elia 1984). Spring peaks in modeled net O₂ production and net DSi uptake in the middle and lower estuary coincided with the typical timing of diatom spring blooms (Figs. 4 & 8) (Fisher et al. 1988, Malone et al. 1988).

Converting net DSi uptake to equivalent carbon units (C:Si = 6.625; Redfield 1958) suggests diatom photosynthesis comprises 50 to 80% of net O₂ production during spring, whereas net production of DSi, which occurs in summer in all regions of the estuary, indicates temperature-stimulated dissolution of silica minerals (Yamada & D'Elia 1984).

Strong seasonal patterns of modeled surface-layer DIN uptake rates were observed throughout the estuary, with spring peaks consistent with high rates of modeled net O₂ production and DSi uptake. Assuming an O₂:N ratio of 6.625, the DIN uptake expected from modeled net O₂ production accounted for 80% of the modeled net DIN uptake in the middle and lower estuary during February to March, but <50% in May and June. The difference between modeled net DIN consumption and the stoichiometric-equivalent DIN uptake associated with net O₂ production reflects the balance between denitrification and nitrogen fixation (Smith et al. 1991). This computed 'net denitrification' in the middle and lower estuary during spring and summer suggests loss of DIN via denitrification in sediments along the estuarine flanks at rates of 75 to 125 μmol N m⁻² h⁻¹, which agree favorably with measured values (e.g. Jenkins & Kemp 1984).

O₂ versus DIP as measures of net ecosystem production

Coupling between modeled net O₂ and DIP production was less direct and consistent than for other variables. Box-model computations of net DIP production have been effectively used to estimate net ecosystem production in several systems (e.g. Smith et al. 1991, Gordon et al. 1996), but O₂ may be a better variable at smaller spatial scales for turbid estuaries like the Patuxent with strong salinity gradients. For example, DIP biogeochemistry may be largely controlled by non-biological processes, such as sorption (Froelich 1988) and flocculation (Sholkovitz 1976). Analyses of seasonal behavior of surface-layer rates in the mesohaline estuary (Boxes 3 to 5) reveal that modeled net O₂ production and DIP uptake were comparable from June to December, but not in winter and spring, where rates of net O₂ production expected from modeled net DIP uptake (assuming O₂:DIP = 106) were 25 to 50% of modeled net O₂ production. Timing of these discrepancies coincides with seasonal maxima in modeled net O₂ production, chl *a*, and TSS. Because DIP desorbs rapidly from particles to replace biologically assimilated ions (Froelich 1988), changes in DIP concentrations at the monthly and regional scales of this analysis might fail to capture this high biological variability. Indeed, the particulate phosphorus pool dominates

(>80%) total water column P from January to May in estuarine regions (www.chesapeakebay.net). In addition, our computations may fail to capture all variability in the bioavailable P fraction, as DOP may be an important component of soluble reactive P (e.g. Gazeau et al. 2005). Modeled net O₂ uptake and DIP production in the oligohaline estuary were highly correlated year-round, but DIP production rates were 80% lower than expected from net O₂ uptake. The waters in this region are relatively shallow, connected to sediments, and net heterotrophic, thus DIP released from organic matter oxidation would tend to bind to iron complexes in oxic sediments (Rozan et al. 2002). Because this region is also characterized by high concentrations of suspended inorganic particles, a large fraction of DIP may be sorbed to these particles, thereby damping changes in DIP associated with biological processes.

Using modeled net O₂ production as a measure of net ecosystem production (Caffrey 2003) also has limitations; we were able to address directly two potential problems associated with this approach. We corrected instantaneous measurements of O₂ to equivalent 24 hr mean values considering systematic diel variations associated with photosynthesis and respiration and found that this correction altered the O₂ concentration by <5%. We also corrected modeled surface-layer net O₂ production rates for air–water exchange and found that variation in the exchange coefficient (α) of $\pm 50\%$ resulted in small changes in net O₂ production (5 to 10% in the middle and lower estuary [Boxes 3 to 6] and 5 to 15% in the upper estuary [Boxes 1 to 2]). Our estimates of net O₂ production, however, agree well with the regional variation, magnitude, and seasonality of previous computations for Chesapeake Bay using a range of different techniques (Smith & Kemp 1995, Kemp et al. 1997). Although modeled bottom-layer net O₂ uptake represents a reasonable index of aerobic and anaerobic respiration (via re-oxidation of sulfide derived from sulfate reduction [SR]; Cornwell & Sampou 1995), there may be a lag between sulfide production and re-oxidation that is greater than a month (the scale of our computations). Apart from long term burial (<10% of SR; Roden et al. 1995), however, the sulfide produced via SR diffuses into overlying water to consume O₂ within a year.

Spatial and temporal patterns of pelagic–benthic coupling

Coincident spring peaks of chl *a* and modeled POC sinking and net diatom growth support the view that diatom blooms comprise most of the spring vertical particle flux (Malone et al. 1988) and that a large frac-

tion of the spring bloom is ungrazed (Kannevorff & Christensen 1986). Diverse studies in temperate systems have reported spring peaks in POC deposition, suggesting that sinking is the dominant loss term for phytoplankton blooms in spring (Smetacek et al. 1978). Box-model computed POC settling velocities during winter–spring agree with measured rates for many larger diatoms (Bienfang 1981).

Vertical sinking of POC provides a mechanism by which surface-layer net production is transported to bottom layers, and box-model computed POC sinking rates for the mesohaline estuary compare favorably with data from sediment trap deployments at nearby sites (Kemp & Boynton 1984, Roden et al. 1995). Comparative analyses of model-computed annual mean rates of surface-layer net O₂ production, bottom-layer net O₂ uptake, and POC sinking, as well as measured chl *a*, revealed that pelagic and benthic processes were tightly coupled in the middle region, but more weakly connected in other areas of the Patuxent. This regional difference may result from the middle region's relatively shallower depths, longer water residence time, and greater isolation of the middle regions relative to other areas of the Patuxent (Hagy et al. 2000).

Positive net O₂ production in surface layers indicated that excess organic production was exported to and respired in adjacent regions (Kemp et al. 1997). Significant correlations between modeled annual rates of surface-layer net O₂ production and underlying bottom-layer net O₂ uptake in the middle estuary suggest that this excess organic production tends to be exported vertically in most years (Fig. 9). Correlations between surface chl *a* and modeled POC sinking with modeled bottom-layer net O₂ uptake in the middle estuary suggest phytoplankton drive organic production and subsequent vertical carbon export, which has been inferred from measured rates in other estuaries (Lignell et al. 1993).

Seasonal mismatch between POC sinking and bottom-layer respiration

Although annual means of modeled POC sinking and bottom-layer net O₂ uptake correlate strongly in the middle estuary, seasonal trends in POC concentration and sinking do not match with those of net O₂ uptake. A large fraction of POC appeared to sink in spring (February to April), but summer (May to September) peaks computed for bottom-layer net O₂ uptake (Fig. 4) indicate that fresh organic matter may not be immediately respired in this system, but consumed later as temperature increases (Cowan et al. 1996). Rates of sediment O₂ uptake measured in the Patuxent

using benthic chambers also peaked 2 mo after the seasonal POC sinking maxima (Boynton & Rohland 2001). However, early summer maxima in bottom-layer net O₂ uptake found throughout the estuary preceded the temperature maximum by 1 mo or more (Fig. 4), suggesting that respiration in this system will respond to recently deposited material (Graf et al. 1982, Fisher et al. 1982), as well as increasing temperature. A multiple regression using contemporaneous temperature and the previous month's bottom-layer chl *a* explained 40% more of the variability ($r^2 = 0.74$ vs. 0.35) in bottom-layer net O₂ uptake than a regression of temperature versus respiration (Hagy 1996). Thus, the respiration of labile organic matter in bottom layers of this estuary is modulated by both temperature and the timing of downward transport of organic matter.

Organic carbon sources for bottom-layer respiration: role of shallow water production

Independent calculations of POC sinking and bottom-layer net O₂ uptake were converted to equivalent C rates (assuming the respiratory quotient = 1.0, Hopkinson 1985) to estimate what fraction of bottom-layer net O₂ uptake was attributable to direct POC sinking from the overlying surface layer. Because the surface layer overlies both the bottom water confined to the central estuarine channel and bottom sediments of the shallow flanks, the surface layer is wider than the bottom layer. Thus, all of the POC sinking from the surface layer may not reach the central bottom layer. Here, we consider two contrasting assumptions. If we assume, on the one hand, that POC sinking is vertical and uniformly distributed, it would settle from surface to bottom layer only where the two overlap (25% of the area in the middle estuary, Table 1), and POC sinking would account for only 20 to 50% of the annual organic C input needed to support modeled bottom-layer net O₂ uptake. On the other hand, if we assume that the entire POC sinking flux was transported to the bottom layer, modeled POC sinking would be sufficient to support 80 to 150% of annual net O₂ uptake. The latter assumption requires that all organic particles settling over the flanks were transported laterally down-slope toward the central channel's lower layer (e.g. Kemp et al. 1997). Because a fraction of upper layer production is buried or incorporated into biomass, it is unlikely that all of this production is transported laterally to the deep channel and the actual coupling between surface and bottom layers is likely somewhere between these 2 contrasting conditions (i.e. 50 to 100%). Although vertical POC sinking rates have been linked to measured benthic respiration rates (e.g. Kamp-Nielsen 1992), this study suggests that a portion of the organic matter

produced in shallow water (<6 m) is transported laterally to support deep, bottom-layer respiration.

Our calculations suggest that surface-layer POC is occasionally insufficient to provide the carbon necessary to support bottom-layer net O₂ uptake. Deficits in POC input to benthos have also been reported for other systems where horizontal transport was a suggested additional organic source (Graf et al. 1982). In the Patuxent estuary, landward transport via gravitational circulation is a likely alternative carbon source (Kemp et al. 1997). Computed rates for net longitudinal transport (input-output) of organic carbon to the bottom layers of the middle and lower estuarine regions ranged from 5 to 30 mmol C m⁻² d⁻¹, which is ~25% of POC sinking rates. Organic carbon transported longitudinally to the bottom layer, however, likely originated as production in seaward surface layers, making it older and less labile than locally produced organic matter. Vertical and lateral POC transport mechanisms thus dominate carbon fluxes to bottom waters in this estuary.

Pelagic–benthic coupling: factors driving nutrient regeneration

Box-model calculations suggest that vertical transport of organic carbon from surface to bottom layers is closely linked to nutrient regeneration in bottom layers of the middle estuary. Correlations for annual mean rates of modeled net bottom-layer DSi production versus both annual mean surface chl *a* ($r^2 = 0.61$) and modeled spring POC sinking ($r^2 = 0.35$) suggests that sinking diatoms are a key source of biogenic silica (Yamada & D'Elia 1984) and that surface production and bottom-layer DSi regeneration are linked (Cowan & Boynton 1996). Similar correlations for annual means of both chl *a* and modeled spring POC sinking rates versus modeled net bottom-layer production of NH₄⁺ ($r^2 = 0.34, 0.25$ respectively, $p < 0.05$) and DIP ($r^2 = 0.31, 0.55$ respectively, $p < 0.05$) also reflect tight coupling between nutrient regeneration and surface phytoplankton growth (Nixon 1981, Cowan et al. 1996). Because modeled POC sinking accounted for 50 to 90% of modeled bottom-layer net regeneration of NH₄⁺, DIP, and DSi, we suggest that nutrients generated in the bottom layer in summer are predominantly derived from the previous spring's production, rather than from long-term accumulation of sediment nutrients (Boynton & Kemp 2000). Similar links have been shown using direct instantaneous measurements of nutrient regeneration and phytoplankton productivity or POC sinking in coastal systems (e.g. Jensen et al. 1990). Unlike box-model-computed rates, however, instantaneous measurements at

fixed sites may not reflect rates integrated over broader time/space scales.

Summer peaks in bottom-layer biogeochemical processes indicate the role of temperature in controlling bottom-layer net O_2 uptake and nutrient recycling. Seasonal coherence between modeled net nutrient regeneration and net O_2 uptake in bottom layers during summer is not only consistent with the enhancement of bacterial respiration rates and enzyme activity by elevated temperature (Fisher et al. 1982, Kamp-Nielsen 1992), but also diagenetic coupling between organic matter decomposition and nutrient regeneration (Kelly et al. 1985, Cowan & Boynton 1996). Although we related the magnitude of modeled net nutrient regeneration in the bottom layer to modeled POC sinking, the timing of regeneration is primarily controlled by temperature-dependent processes, including chemical dissolution (e.g. DSi; Yamada & D'Elia 1984), shifts in redox conditions (e.g. DIP; Rozan et al. 2002), and enzyme catalyzed hydrolysis (e.g. NH_4^+ , O_2 ; Cowan & Boynton 1996).

Seasonal variability in nitrogen sources fueling surface-layer productivity

In temperate estuaries, the traditional paradigm asserted that 'new' organic production in spring was supported by watershed nutrient inputs, while summer production was fueled by nutrients recycled from organic matter deposited into the bottom layer during spring (e.g. Kemp & Boynton 1984, Malone et al. 1988). Because the patterns observed in many estuaries are not so distinct, we used the box-model to quantify DIN transport at seasonal and regional scales. Our analysis of the Patuxent estuary indicates that, consistent with previous suggestions, seaward transport of DIN is sufficient to support >100% of spring phytoplankton production (as reflected in net O_2 production) in the middle and lower estuary, while vertical fluxes of DIN (mostly NH_4^+) from bottom to surface layers tend to be large enough to satisfy 70 to 80% of net summertime DIN uptake computed for the surface layer (Fig. 10). Vertical DIN fluxes are supported by bottom-layer DIN regeneration (Hagy 1996) and because this annual mean DIN production is tightly linked to spring POC sinking, we can infer the coupling of spring N inputs to summer regeneration. Support of summer phytoplankton productivity by sediment NH_4^+ fluxes has been inferred from core or chamber measurements in other temperate estuaries (Fisher et al. 1982). The additional 20 to 30% of N inputs during summer are probably derived from upstream sources, atmospheric inputs, or internal pelagic recycling processes (Suttle et al. 1990). In the lower estuary, over 100% of the surface-layer

net DIN demand could be supported by seaward DIN transport in all seasons. A substantial fraction of this DIN transported seaward from the upper to the lower estuary during summer, however, is derived from vertical inputs of NH_4^+ from bottom waters in upstream regions. Indeed, NH_4^+ comprised 60 to 80% of seaward DIN transport to the lower estuary during summer and seaward NH_4^+ transport increased linearly from Box 1 to Box 5. This cumulative increase in solutes mixed vertically from bottom to surface waters is driven by 2-layer gravitational circulation (e.g. Dyer 1974, Hagy et al. 2000) and it is supported by nutrient regeneration from both bottom water and sediment processes (Testa 2006). This analysis provides quantitative support for the concept that high spring DIN inputs generate net organic production that sinks to the lower layer, where DIN is regenerated in summer and transported upward to support primary productivity in many shallow temperate estuaries (Kemp & Boynton 1984, Malone et al. 1988). We emphasize, however, that DIN regenerated in bottom water may be transported both vertically and horizontally before it is assimilated.

Effects of river flow on surface- and bottom-layer biogeochemistry

Variation in river flow can exert a strong influence on phytoplankton biomass and productivity via the processes of nutrient inputs, allochthonous inputs, stratification, and residence time. In many estuaries, increased phytoplankton productivity and biomass are often associated with high river flow (Malone et al. 1988). This occurred in the middle and lower Patuxent estuary (Figs. 6 & 7) where modeled surface-layer rates of net O_2 production and DIN uptake, along with measured chl *a*, were generally elevated during high flow years, especially during summer (Fig. 6). It appears that the primary mechanism for this stimulation is attributable to increased nutrient inputs at high river flow (Boynton & Kemp 2000), particularly during summer when nutrient limitation is most pronounced (Fisher et al. 1988). Conversely, chl *a* and modeled rates of net O_2 production decreased during high flow in the upper estuary because of increased turbidity and flushing rates (Cloern et al. 1983).

Despite the significant positive effects of river flow on surface biomass and productivity in the mesohaline estuary, our analysis suggests that POC sinking and modeled rates of bottom-layer net O_2 uptake and nutrient regeneration were less responsive to variations in river flow (Fig. 7). Previous studies in Chesapeake Bay have reported increased rates of chl *a* deposition and increased sediment NH_4^+ regeneration during high flow (Boynton & Kemp 2000), but the lack of significant

relationships between river flow and net biogeochemical rates in bottom layers of the Patuxent may be attributable to enhanced seaward advective transport in the estuary's surface layer under high flow conditions. In this case, much of the excess primary production in wet years tends to be swept seaward out of estuarine regions rather than sinking vertically to the underlying bottom layer (Hagy et al. 2005) because the Patuxent is a much smaller system than Chesapeake Bay. Indeed, surface-layer seaward advective rates calculated with the box-model reveal that seaward POC transport (out of each box) is 30 to 45 % higher in wet years compared to dry years.

Here we have presented a range of scientific questions that we were able to address using box-model computations; however, an even broader scope of specific or generic questions could be investigated with this approach, particularly in estuarine systems with 2-layered circulation. The approach is limited, however, in that only net rates can be computed, so that the many specific processes contributing to these net rates cannot be quantified separately. Related approaches have already been applied at various scales in many systems throughout the world (e.g. Wulff & Stigebrandt 1989, Smith et al. 1991, Gazeau et al. 2005, Bozec et al. 2006), but the full interpretive power of these computations has seldom been exploited. Ultimately, however, this technique has potential to provide an integrative approach for addressing both fundamental research questions and critical management problems in diverse coastal ecosystems.

Acknowledgements. We thank J. D. Hagy for help with SAS programming, discussions of box-modeling, and many useful comments on earlier drafts. We also thank L. Sanford and W. R. Boynton for critical reviews of previous drafts and many helpful suggestions. Many individuals provided advice and contributed data or assistance to this research, including J. Apple, L. Codispoti, L. W. Harding, V. Kelly, D. Kimmel, and W. D. Miller. This work was funded by a Horn Point Laboratory Graduate Research Fellowship and a NOAA National Estuarine Research Reserve System (NERRS) Graduate Research Fellowship to J.M.T. This is contribution no. 4125 from the University of Maryland Center for Environmental Science.

LITERATURE CITED

- Bienfang PK (1981) Sinking rates of heterogeneous, temperate phytoplankton populations. *J Plankton Res* 3:235–253
- Boynton WR, Kemp WM (2000) Influence of river flow and nutrient loads on selected ecosystem processes: a synthesis of Chesapeake Bay data. In: Hobbie JE (ed) *Estuarine science, a synthetic approach to research and practice*. Island Press, Washington, DC, p 269–298
- Boynton WR, Rohland FM (2001) Maryland Chesapeake Bay Water Quality Monitoring Program, Ecosystem Processes Component, Level One Report no. 18. Ref. no. [UMCES]CBL 01-0088, Maryland Department of Natural Resources, Annapolis, MD
- Bozec Y, Thomas H, Schiettecatte LS, Borges AV, Elkalay K, de Baar HJW (2006) Assessment of the processes controlling seasonal variations of dissolved inorganic carbon in the North Sea. *Limnol Oceanogr* 51:2746–2762
- Caffrey JM (2003) Production, respiration, and net ecosystem metabolism in US estuaries. *Environ Monit Assess* 81: 207–219
- Cloern JE, Alpine AE, Cole BE, Wong RLJ, Arthur JF, Ball MD (1983) River discharge controls phytoplankton dynamics in the northern San Francisco Bay Estuary. *Estuar Coast Shelf Sci* 16:415–429
- Cornwell JC, Sampou PA (1995) Environmental controls on iron sulfide mineral formation in a coastal plain estuary. In: Vairamurthy MA, Schoonen MAA (eds) *Geochemical transformations of sedimentary sulfur*. American Chemical Society, Washington, DC, p 224–242
- Cowan JL, Boynton WR (1996) Sediment-water oxygen and nutrient exchanges along the longitudinal axis of Chesapeake Bay: seasonal patterns, controlling factors and ecological significance. *Estuaries* 19:562–580
- Cowan JLW, Pennock JR, Boynton WR (1996) Seasonal and interannual patterns of sediment-water nutrient and oxygen fluxes in Mobile Bay, Alabama (USA): regulating factors and ecological significance. *Mar Ecol Prog Ser* 141: 229–245
- Dyer KR (1974) The salt balance in stratified estuaries. *Estuar Coast Mar Sci* 2:273–281
- Fisher TR, Carlson PR, Barber RT (1982) Sediment nutrient regeneration in three North Carolina estuaries. *Estuar Coast Shelf Sci* 14:101–116
- Fisher TR, Harding LW Jr, Stanley DW, Ward LG (1988) Phytoplankton, nutrients, and turbidity in the Chesapeake, Delaware, and Hudson estuaries. *Estuar Coast Shelf Sci* 27:61–93
- Froelich PN (1988) Kinetic control of dissolved phosphate in natural rivers and estuaries: a primer on the phosphate buffer mechanism. *Limnol Oceanogr* 33:649–668
- Gazeau F, Gattuso JP, Middelburg JJ, Brion N, Schiettecatte LS, Frankignoulle M, Borges AV (2005) Planktonic and whole system metabolism in a nutrient-rich estuary (the Scheldt Estuary). *Estuaries* 28:868–883
- Gordon DC Jr, Boudreau PR, Mann KH, Ong JE and others (1996) LOICZ biogeochemical modeling guidelines. LOICZ Reports and Studies no. 5, LOICZ, Texel
- Graf G, Berngtsson W, Diesner U, Shultz R, Theede H (1982) Benthic response to sedimentation of a spring phytoplankton bloom: process and budget. *Mar Biol* 67:201–208
- Hagy JD (1996) Residence times and net ecosystem processes in the Patuxent River estuary. MSc Thesis, University of Maryland at College Park, MD
- Hagy JD, Sanford LP, Boynton WR (2000) Estimation of net physical transport and hydraulic residence times for a coastal plain estuary using box models. *Estuaries* 23: 328–340
- Hagy JD, Boynton WR, Jasinski DA (2005) Modeling phytoplankton deposition to Chesapeake Bay sediments during winter-spring: interannual variability in relation to river flow. *Estuar Coast Shelf Sci* 62:25–40
- Harding LW, Mallonee ME, Perry E (2002) Toward a predictive understanding of primary productivity in a temperate, partially stratified estuary. *Estuar Coast Shelf Sci* 55: 437–463
- Heath M (1995) An holistic analysis of the coupling between physical and biological processes in the coastal zone. *Ophelia* 42:95–125

- Hopkinson CS (1985) Shallow-water benthic and pelagic metabolism: evidence of heterotrophy in the nearshore Georgia Bight. *Mar Biol* 87:19–32
- Hoppema JM (1991) The oxygen budget of the western Wadden Sea, The Netherlands. *Estuar Coast Shelf Sci* 32: 483–502
- Howarth RW, Schneider R, Swaney D (1996) Metabolism and organic carbon fluxes in the tidal freshwater Hudson River. *Estuaries* 19:848–865
- Jenkins MC, Kemp WM (1984) The coupling of nitrification and denitrification in two estuarine sediments. *Limnol Oceanogr* 29:609–619
- Jensen MH, Lomstein E, Sørensen J (1990) Benthic NH_4^+ and NO_3^- flux following sedimentation of a spring phytoplankton bloom in Aarhus Bight, Denmark. *Mar Ecol Prog Ser* 61:87–96
- Kamatani A, Riley JP (1979) Rate of dissolution of diatom silica walls in seawater. *Mar Biol* 55:29–35
- Kamp-Nielsen L (1992) Benthic-pelagic coupling of nutrient metabolism along an estuarine eutrophication gradient. *Hydrobiologia* 235/236:457–470
- Kanneworff E, Christensen H (1986) Benthic community respiration in relation to sedimentation of phytoplankton in the Oresund. *Ophelia* 26:269–284
- Kelly JR, Berounsky VM, Nixon SW, Oviatt CA (1985) Benthic-pelagic coupling and nutrient cycling across an experimental eutrophication gradient. *Mar Ecol Prog Ser* 26: 207–219
- Kemp WM, Boynton WR (1984) Spatial and temporal coupling of nutrient inputs to estuarine primary production: the role of particulate transport and decomposition. *Bull Mar Sci* 35:522–535
- Kemp WM, Smith EM, Marvin-DiPasquale M, Boynton WR (1997) Organic carbon balance and net ecosystem metabolism in Chesapeake Bay. *Mar Ecol Prog Ser* 150:229–248
- Kemp WM, Batiuk R, Bartleson R, Bergstrom P and others (2004) Habitat requirements for submerged aquatic vegetation in Chesapeake Bay: water quality, light regime, and physical-chemical factors. *Estuaries* 27:363–377
- Kocum E, Underwood GJC, Nedwell DB (2002) Simultaneous measurement of phytoplanktonic primary production, nutrient and light availability along a turbid, eutrophic UK east coast estuary (the Colne Estuary). *Mar Ecol Prog Ser* 231:1–12
- Lignell R, Heiskanen AS, Kuosa H, Gundersen K, Kuoppo-Leinikki P, Pajuniemi R, Uitto A (1993) Fate of a phytoplankton spring bloom: sedimentation and carbon flow in the planktonic food web in the northern Baltic. *Mar Ecol Prog Ser* 94:239–252
- Linker LC, Stigall CG, Chang CH, Doingian AS Jr (1996) Aquatic accounting: Chesapeake Bay watershed model quantifies nutrient loads. *Water Environ Technol* 8:48–52
- Malone TC, Crocker LH, Pike SE, Wendler BW (1988) Influences of river flow on the dynamics of phytoplankton production in a partially stratified estuary. *Mar Ecol Prog Ser* 48:235–249
- Marino R, Howarth RW (1993) Atmospheric oxygen exchange in the Hudson River: dome measurements and comparison with other natural waters. *Estuaries* 16:433–445
- Nixon SW (1981) Remineralization and nutrient cycling in coastal marine ecosystems. In: Neilson BJ, Cronin LE (eds) *Estuaries and nutrients*. Humana Press, Clifton, NJ, p 111–138
- Officer CB (1980) Box models revisited. In: Hamilton P, Macdonald RB (eds) *Estuarine and wetland processes*. Plenum Press, New York, p 65–114
- Pennock JR, Sharp JH (1994) Temporal alteration between light- and nutrient-limitation of phytoplankton production in a coastal plain estuary. *Mar Ecol Prog Ser* 111:275–288
- Pritchard DW (1969) Dispersion and flushing of pollutants in estuaries. *J Hydraul Div ASCE* 95(HY1):115–124
- Radach G, Berg J, Hagmeier E (1990) Long-term changes of the annual cycles of meteorological, hydrographic, nutrient and phytoplankton time series at Helgoland and LV ELBE 1 in the German Bight. *Cont Shelf Res* 10:305–328
- Redfield AC (1958) The biological control of chemical factors in the environment. *Am Sci* 46:205–221
- Roden EE, Tuttle JH, Boynton WR, Kemp WM (1995) Carbon cycling in mesohaline Chesapeake Bay sediments. 1. POC deposition rates and mineralization pathways. *J Mar Res* 53:779–819
- Rozan TF, Taillefert M, Trouwborst RE, Glazer BT and others (2002) Iron-sulfur-phosphorus cycling in the sediments of a shallow coastal bay: implications for sediment nutrient release and benthic macroalgal blooms. *Limnol Oceanogr* 47:1346–1354
- Sholkovitz ER (1976) Flocculation of dissolved organic and inorganic matter during the mixing of river water and seawater. *Geochim Cosmochim Acta* 40:831–845
- Smetacek VK, Von Brockel K, Zeitzschel B, Zenk W (1978) Sedimentation of particulate matter during a phytoplankton spring bloom in relation to hydrographical regime. *Mar Biol* 47:211–226
- Smith SV, Hollibaugh JT (1997) Annual cycle and interannual variability of net ecosystem metabolism in a temperate climate embayment. *Ecol Monogr* 67:509–533
- Smith EM, Kemp WM (1995) Seasonal and regional variations in plankton community production and respiration for Chesapeake Bay. *Mar Ecol Prog Ser* 116:217–231
- Smith SV, Hollibaugh JT, Dollar SJ, Vink S (1991) Tomales Bay metabolism C-N-P stoichiometry and ecosystem heterotrophy at the land-sea interface. *Estuar Coast Shelf Sci* 33:223–257
- Suttle CA, Fuhrman JA, Capone DG (1990) Rapid ammonium cycling and concentration-dependent partitioning of ammonium and phosphate: implications for carbon transfer in planktonic communities. *Limnol Oceanogr* 35: 424–433
- Testa JM (2006) Factors regulating variability in water quality and net biogeochemical fluxes in the Patuxent River estuary. MSc Thesis, University of Maryland at College Park, College Park, MD
- Vannote RL, Minshall GW, Cummins KW, Sedwell JR, Cushing CE (1980) The river continuum concept. *Can J Fish Aquat Sci* 37:130–137
- Williams MR, Fisher TR, Boynton WR, Cerco CF and others (2006) An integrated modelling system for management of the Patuxent River estuary and basin, Maryland, USA. *Int J Remote Sens* 27:3705–3726
- Wulff F, Stigebrandt A (1989) A time-dependent budget model for nutrients in the Baltic Sea. *Global Biogeochem Cycles* 3:63–78
- Yamada SS, D'Elia CF (1984) Silicic acid regeneration from estuarine sediment cores. *Mar Ecol Prog Ser* 18:113–118